

# Feature-Filter: Detecting Adversarial Examples through Filtering off Recessive Features

Hui Liu, Bo Zhao, Yuefeng Peng, Jiabao Guo, and Peng Liu, *Member, IEEE*

**Abstract**—Deep neural networks (DNNs) are under threat from adversarial example attacks. The adversary can easily change the outputs of DNNs by adding small well-designed perturbations to inputs. Adversarial example detection is a fundamental work for robust DNNs-based service. Adversarial examples show the difference between humans and DNNs in image recognition. From a human-centric perspective, image features could be divided into dominant features that are comprehensible to humans, and recessive features that are incomprehensible to humans, yet are exploited by DNNs. In this paper, we reveal that imperceptible adversarial examples are the product of recessive features misleading neural networks, and an adversarial attack is essentially a kind of method to enrich these recessive features in the image. The imperceptibility of the adversarial examples indicates that the perturbations enrich recessive features, yet hardly affect dominant features. Therefore, adversarial examples are sensitive to filtering off recessive features, while benign examples are immune to such operation. Inspired by this idea, we propose a label-only adversarial detection approach that is referred to as feature-filter. Feature-filter utilizes discrete cosine transform to approximately separate recessive features from dominant features, and gets a mutant image that is filtered off recessive features. By only comparing DNN’s prediction labels on the input and its mutant, feature-filter can real-time detect imperceptible adversarial examples at high accuracy and few false positives.

**Index Terms**—Deep neural networks, adversarial example, dominant features, recessive features, discrete cosine transform.

## I. INTRODUCTION

**D**EEP neural networks (DNNs) [1]–[4] achieve state-of-the-art performance on many artificial intelligence tasks, including safety-critical systems like facial biometric systems [5], intrusion detection system [6], etc. However, a large number of studies have shown that attackers can easily change the outputs of DNNs by the inputs with well-designed perturbations (adversarial examples) [8]. The malicious action is called “adversarial attack” [9], [11]–[17].

Adversaries could modify any pixel value in the image to generate adversarial examples. In the physical world, however, they don’t want modifications that can easily irritate the human eye. For example, autonomous vehicles deploy extensive neural networks to construct their perceptual systems [18], [19]. Adversaries could try to affect the decision-making of perceptual systems by using adversarial traffic signs. If these modifications in traffic signs can be easily detected by the

human eye, the traffic police would replace them in time and the adversarial attack would fail before it had even begun. Therefore, in order to achieve this goal, adversaries must ensure that these modifications are imperceptible to the human eye. This constraint of imperceptibility is widespread in real-world scenarios.

The phenomenon of adversarial examples has attracted a great number of interests in the research community in recent years. To hardening DNN systems, A wide range of proactive defense approaches [20]–[24] have been proposed in image classification, but those defenses can be evaded by emerging attack approaches [25]. If there are no known intrinsic properties that distinguish adversarial examples from benign examples, these proactive adversarial defenses are extremely challenging [26].

As a fundamental work for robust DNNs, detecting adversarial examples may be as important as adversarial defenses. Adversarial detection aims to distinguish adversarial examples from benign ones by intrinsic properties. To discover these intrinsic properties, let us analyze the reasons for the existence of imperceptible adversarial examples in the image recognition.

There has been a debate on why the adversarial examples exist. Previous work has proposed several explanations for the phenomenon of adversarial examples, ranging from finite-sample overfitting to high-dimensional statistical properties [27]–[29]. However, Andrew et al. [30] argued these theories were often unable to fully capture behaviors, and first categorized image features from a human-centric perspective. Inspired by this study, we observe that adversarial examples show the difference between humans and DNNs in the utilization of input features. For accurate classification, DNNs make full use of the input features, of which spaces are often unnecessarily large for humans. The human eyes recognize images only according to those features that are comprehensible to humans. As a human-centric phenomenon, the input features could be divided into two categories: dominant features that are comprehensible to humans, and recessive features that are incomprehensible to humans. When adversarial perturbations enough enrich recessive features and hardly lose dominant features, they would mislead the output of DNNs and not result in noticeable artifacts to the human eyes. Thus, we claim that the existence of imperceptible adversarial examples is due to the neural network’s use of these recessive features.

Since adversarial examples generated by state-of-the-art attack approaches have rich recessive features to mislead DNN models, they would be much more sensitive to filter off these recessive features than benign examples. A natural detection strategy of adversarial examples is driven by comparing the

H. Liu, B. Zhao, Y. Peng, J. Guo are with the School of Cyber Science and Engineering, Wuhan University, Wuhan, 430072 China e-mail: zhaobo@whu.edu.cn.

P. Liu is with the College of Information Sciences and Technology, Pennsylvania State University, PA, 16801 US e-mail: pliu@ist.psu.edu.

Manuscript received Oct. 29, 2020.

model’s predictions on the original input and its mutant that is filtered off recessive features, as depicted in Figure 1. Where, the filter filters off recessive features of the original image as a mutant image. If the original image and the mutant image are classified by the DNN model into different categories, this image would be judged as an adversarial example.

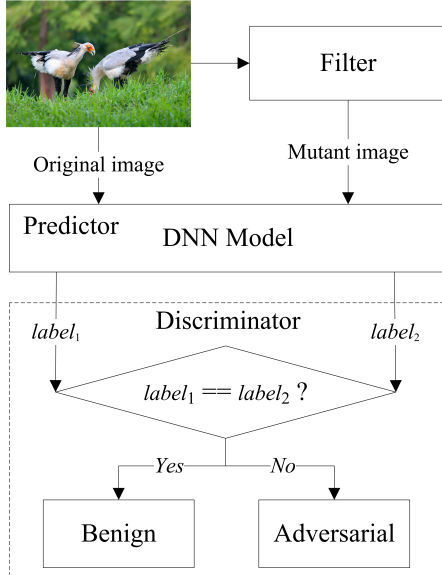


Fig. 1: Adversarial Example Detection Framework Based on Feature Filtering.

A challenging task is how to reliably filter off the recessive features from the original image. A key idea is inspired by classical JPEG compression based on discrete cosine transform (DCT) [31]–[33]. As depicted in Figure 2, the compressed image is still clearly recognizable to humans, even though the feature space is only 1/10 the size of the original image. It indicates that a large number of dominant features are retained, and the contents filtered off almost exclusively include recessive features. Therefore, DCT could be employed as the filter in Figure 1 to filter off recessive features from input features.

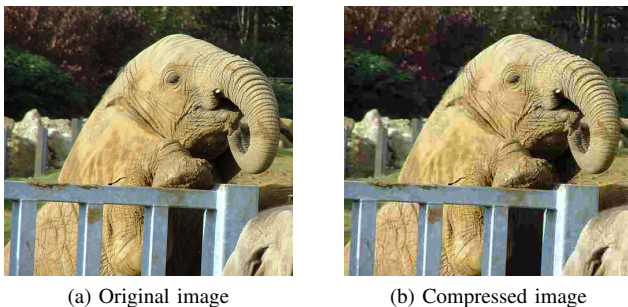


Fig. 2: Images based on JPEG compression.

In summary, this paper makes the following contributions:

- We analyze the reason for the existence of imperceptible adversarial examples, and reveal that the imperceptible adversarial example is the product of abundant recessive features misleading neural networks.

- To clarify the above explanation, we propose a label-only adversarial detection approach that is referred as feature-filter. Feature-filter can identify adversarial examples by only comparing prediction labels of the DNN on the original image and its mutant image.
- We design a DCT-based filter to filter off recessive features of the image. The experiments verify that DCT is a reliable tool to separate recessive features from dominant features.

The remainder of this paper is organized as follows. Section II introduces the related work about adversarial attacks, defenses and detections. Section III is the preliminaries about the proposed detection. In Section IV, we give details about the design and the implementation of the feature-filter. Section V evaluates the performance of the DCT-based filter and our detector. Finally, we conclude the paper in Section VI.

## II. RELATED WORK

In this section, we briefly review existing works on adversarial attacks, defenses and detections.

**Adversarial attacks:** The adversarial example is first discovered in exploring properties of neural networks. Szegedy et al. [8] found that the DNN would misclassify a well-designed image, in which certain perturbations were hardly perceptible to the human eyes. They designed a box-constrained L-BFGS to compute an approximate minimum perturbation matrix.

Many improved works have been subsequently proposed by modifying the adversarial objective function. For example, the fast gradient sign method (FGSM) [9] updates each pixel along the direction of the sign of gradient and performs a fast one-step attack. The fast gradient value method (FGVM) [10] replaces the sign of the gradient with the raw gradient, and generates adversarial examples with a larger local difference. Despite their efficiency, these methods provides only a coarse approximation of the optimal perturbations, resulting in unnecessarily large artifacts.

To improve the imperceptibility of perturbations, DeepFool [12] designed an accurate method by moving the input image across its closest decision boundary. Adversarial examples generated by DeepFool have less perturbations in the input image than those generated by L-BFGS and FGSM. Inspired by DeepFool, an universal adversarial attack [13] was proposed to reveal important geometric correlations among the high-dimensional decision boundary of DNNs, which proved the transferability of adversarial examples across neural networks.

Among existing adversarial attacks, C&W [25] attack performs high resilience against the most defense and detection methods. Especially,  $L_2$  attack among them is argued to be the most effective to date in white-box threat model. Therefore, most adversarial detectors are evaluated by testing in adversarial examples generated by C&W attack.

**Adversarial defenses:** A wide variety of proactive defense approaches have been proposed to harden the neural network. Based on a comprehensive summary, adversarial defenses are grouped into two broad categories: adversarial training and gradient masking [34].

Adversarial training extends the training dataset by adversarial examples with the ground-truth labels and retrain

the neural network using this extended dataset. Goodfellow et al. [9] claimed that adversarial training could provide an additional regularization benefit and increase the robustness of neural networks. Although this type of defense works against attacks on which the model is trained, it faces potential risks for new attacks.

Gradient masking is an effective defensive strategy against gradient-based adversarial attacks. These attack methods compute first-order derivatives to estimate the sensitivity of the model with respect to inputs. Papernot et al. [35] introduced “defensive distillation” to defend DNNs against adversarial examples. To hide the model’s gradients, network distillation replaces its softmax layer with a “softer” softmax function. In fact, gradients are not essential knowledge for attackers, who easily evade gradient masking using a transferability-based black-box attack [13].

**Adversarial detections:** Due to the difficulty of adversarial defenses, recent works focus on reactive adversarial detections, which distinguish adversarial images from benign images. Adversarial detections could be grouped into three categories: statistical measurement [36]–[38], secondary classifier [39], [40] and input transformation [41]–[44].

Statistical measurement aims to find the statistical differences in the high-dimensional features extracted from DNN layers. NNIF [36] utilized influence functions and nearest neighbors to construct k-NN features, which are employed to train a logistic regression for adversarial detection. ML-LOO [38] computes the contribution of features in the prediction of model to construct feature attribution map, and then measures 3 metrics (standard deviation, median absolute deviation and interquartile range) of statistical dispersion in feature attribution map. The experiments revealed a significant difference in the distributions of 3 metrics between benign and adversarial images. Due to the intrinsically unperceptive nature of adversarial examples, statistical measurement seems unlikely to be effective to detect adversarial examples.

Adversarial detections is essentially binary classification problem. A nature idea is to train secondary classifiers to detect if the input is benign or adversarial. NIC [39] trains a model for each layer in the DNN to describe the distributions of the provenance and the activation value. By combining the results of all models, NIC makes a joint prediction to determine whether the input image is adversarial or not. In fact, the secondary classifiers also could be fooled, thus, they have the potential vulnerability to second-round adversarial attacks.

The basic idea of input transformation is to measure the disagreement of the target model in predicting the input and its mutants. Xu et al. [41] proposed a detection strategy, feature squeezing, to squeeze feature space available to attackers. However, they did not specify which features should be squeezed. Kantaros et al. [43] observed that adversarial examples are sensitive to lossy compression transformations. They proposed VisionGuard to real-time detect large-scale adversarial examples. VisionGuard measured similarity of softmax outputs between the test image and its compressed version using the K-L divergence measure. When the K-L divergence is greater than a threshold, the test image

is considered an adversarial input. VisionGuard determined the detection threshold based on the training dataset and its adversarial dataset, which makes it inapplicable to data with different distributions. Tian et al. [42] exploited a set of rotation operations to yield several transformed versions and analyzed the classification results of these transformed images to determine if the test image is adversarial. Since input transformation can not change neural networks, it is inexpensive and complementary to other defenses and detections.

### III. PRELIMINARIES

#### A. Neural Network

A neural network [1]–[4], [7] has a hierarchical structure, in which each layer is composed of a set of perceptrons. Perceptrons map inputs to output values with a nonlinear activation function, e.g. sigmoid, tanh, and ReLU. The function of a neural network is formed in a chain.

$$f(x, \theta) = f^{(k)}(\dots f^{(2)}(f^{(1)}(x, \theta_1), \theta_2), \theta_k) \quad (1)$$

where  $x$  is the input example and  $\theta_i$  is the weight of the  $i$ 'th layer,  $i = 1, 2, \dots, k$ .  $f^{(i)}(x, \theta_i)$  is the function of the  $i$ 'th layer of the network.

Convolutional neural network is one of the most widely used neural networks, which consists of alternating convolutional layers and pooling layers. Convolutional neural network has performed incredible successes in image recognition. As a representative network, Inception V3 [7] has 23,851,784 parameters and performs 93.70% top-5 accuracy for the ImageNet dataset.

#### B. Adversarial Attack

Adversarial attack [9], [11]–[17] is a unique form of attack in deep learning, in which attackers are able to change DNNs’ outputs by adding imperceptible perturbations to inputs. Adversarial attack would be formulated as an optimization problem with imperceptibility as the main constraint, that is,

$$\begin{aligned} \min \quad & \|\delta\|_p \\ \text{s.t.} \quad & f(x) = l \\ & f(x') = l' \\ & l \neq l' \\ & x' = x + \delta \in D \end{aligned} \quad (2)$$

where  $\delta$  denotes the perturbation matrix that is added to the benign example  $x$  for synthesizing the adversarial example  $x'$ , which remains in the benign domain  $D$ , and a trained DNN model  $f$  predicts  $x$  and  $x'$  into different labels ( $l \neq l'$ ),  $\|\cdot\|$  denotes the distance between two data sample.

Among the state-of-the-art attacks, C&W [25] attacks achieve the best attacking performance comparing with existing-attack algorithms. This set of attacks provide 3 metrics to measure its distortion ( $L_0$ ,  $L_2$  and  $L_\infty$  norms), and  $L_2$  norm is the most powerful attack among them. C&W [25] attacks with  $L_2$  norm could be formulated as follows,

$$\begin{aligned} \min \quad & \|\delta\|_2 + c \cdot \text{Loss}(x') \\ \text{s.t.} \quad & x' = x + \delta \in D \end{aligned} \quad (3)$$

where  $c$  is a hyper-parameter, and  $Loss$  is defined as

$$Loss(x') = \max(\max\{Z(x')_i : i \neq t\} - Z(x')_t, -k) \quad (4)$$

where  $Z(x)$  is the output of the network before the softmax layer, and a hyper-parameter  $k$  encourages the attack to search for an adversarial example  $x'$  that will be classified as label  $t$  with high confidence.

### C. Dataset

1) *CIFAR-10*: The CIFAR-10 dataset consists of 60,000  $32 \times 32 \times 3$  color images in 10 categories, with 6,000 images per category. The dataset is divided into five training batches and one test batch, each with 10,000 images in random order. Due to the low resolution and small category, CIFAR-10 is vulnerable to adversarial attacks, defenses and detections. The dataset is available online at <http://www.cs.toronto.edu/~kriz/cifar.html>.

2) *ImageNet*: ImageNet a large-scale hand-labeled dataset organized according to the WordNet hierarchy. ImageNet Large Scale Visual Recognition Challenge (ILSVRC) has encouraged a lot of mile-stone works and has become the standard benchmark for large-scale object recognition. In ILSVRC2012 ImageNet dataset [45], validation dataset contains 50,000 of high-resolution images in 1,000 categories. Each image usually contains multiple objects, and only one object category is hand-labeled in each image. Therefore, the top-1 and top-5 accuracy is employed to evaluate the model's performance on the ILSVRC2012 validation dataset. The dataset is available online at <http://www.image-net.org/challenges/LSVRC/2012/>.

### D. Image Noise

Image noise is random variation of pixel value in images. The most frequently occurring noises include Gaussian noise, Poisson noise, salt&pepper noise, etc. Gaussian noise is statistical additive noise, which has a probability density function equal to that of the Gaussian distribution. Similarly, Poisson noise is an additive noise, which conforms to the Poisson distribution. The values that the noise can take on are Poisson-distributed. Salt&pepper noise is also known as impulse noise, which replaces random pixels with either 1 or 0. Thus, salt&pepper noise presents itself as sparsely occurring white and black pixels. In this paper, these 3 types of noises are added to benign images to test natural noise detection by the feature-filter.

### E. Discrete Cosine Transform

Discrete cosine transform (DCT) [31]–[33] is a Fourier-like transform, which performs the cosine-series expansion. Due to its high “energy compaction” property, the transformed signal can be easily analyzed using few low-frequency components. Thus, DCT is usually employed to perform decorrelation of the input signal and to present the output in the frequency domain. Among several types of DCT, two-dimensional DCT is the most popular symmetric variation of the transform that

operates on images and its inverse. Two-dimensional DCT of an  $M \times N$  image  $s(x, y)$  are defined as follows.

$$S(\mu, \nu) = \alpha_\mu \alpha_\nu \sum_{x=0}^{M-1} \sum_{y=0}^{N-1} s(x, y) \times \cos\left(\frac{\pi\mu(2x+1)}{2M}\right) \cos\left(\frac{\pi\nu(2y+1)}{2N}\right) \quad (5)$$

The inverse of two-dimensional DCT for an  $M \times N$  sample:

$$s(x, y) = \sum_{\mu=0}^{M-1} \sum_{\nu=0}^{N-1} \alpha_\mu \alpha_\nu S(\mu, \nu) \times \cos\left(\frac{\pi\mu(2x+1)}{2M}\right) \cos\left(\frac{\pi\nu(2y+1)}{2N}\right) \quad (6)$$

The matrix  $S(\mu, \nu)$  is the DCT coefficients of image  $s(x, y)$ , whereas, the basis functions are,

$$\alpha_\mu = \begin{cases} 1/\sqrt{M} & x = 0 \\ \sqrt{2/M} & 0 \leq x \leq M-1 \end{cases} \quad (7)$$

$$\alpha_\nu = \begin{cases} 1/\sqrt{N} & y = 0 \\ \sqrt{2/N} & 0 \leq y \leq N-1 \end{cases}$$

The energy of the image concentrates on the low-frequency DCT components. Human eyes have a poor perception in high-frequency DCT domain. Based on this property, Two-dimensional DCT is widely used in lossy compression [43] and image steganography [46]. In this paper, we apply two-dimensional DCT to availablely filter off recessive features from the image.

## IV. METHODOLOGY

We design a label-only framework that is referred to as feature-filter to detect adversarial examples. Unlike conventional detection approaches which need to calculate the statistical distance between the original image and its transformed image, feature-filter only compares DNN's prediction labels between the input image and its mutant. If prediction labels do not match, it implies that the input image is adversarial. In this section, we give details about feature-filter framework and introduce how to generate the mutant image based on DCT.

### A. Feature-Filter Framework

In order to achieve high imperceptibility, state-of-the-art adversarial attacks attempt to enrich recessive features by adding perturbations into original images, which results in a very significant difference in recessive features between benign images and adversarial images. Therefore, adversarial examples is sensitive to the operation of filtering off recessive features, whereas benign examples are not. That is, if the test image is an adversarial example, the DNN-based classifier would predict it and its mutant without recessive features into different categories. This idea drove us to design an adversarial example detector by comparing DNN's prediction labels.

Feature-filter employs well-established software testing scheme named metamorphic testing to expose adversarial images that lead to inconsistent predictions of the DNN model. As depicted in Figure 1, the feature-filter consists of a filter,

a predictor, and a discriminator, whose functions are shown below.

(1) Filter: Filter off recessive features of the input image and obtain its mutant image;

(2) Predictor: Enter the test image and its mutant image into DNN model  $f$  and obtain the DNN’s prediction labels;

(3) Discriminator: If the test image and its mutant are predicted into the same category, the test image is judged to be benign; otherwise, it is judged to be adversarial.

The implementation of the feature-filter is presented in Algorithm 1. In feature-filter framework, the performance of the proposed detector depends on DNN’s prediction on the mutant image. Therefore, a key problem is how to construct a filter so that it can reliably filter off recessive features from the test image. In the next subsection, the construction of the filter is introduced in detail.

---

**Algorithm 1: The Implementation of the Feature-Filter**

---

**Input:** Test image  $x$   
**Output:** Discriminator( $x$ ) = {True or False}

1	$xm = \text{Filter}(x)$	← Filter off recessive features of the test image $x$ and obtain a mutant image $xm$
2	$pt = f(x)$	← DNN predicts the category of the test image $x$
3	$pm = f(xm)$	← DNN predicts the category of the mutant image $xm$
4	<b>if</b> $pt \neq pm$ <b>then:</b>	← Test image and its mutant are not the same category
5	Discriminator( $x$ ) = True	← Test image is adversarial
6	<b>else:</b>	
7	Discriminator( $x$ ) = False	← Test image is benign
8	<b>end if</b>	

---

### B. Filter Based on DCT

This section describes how we design a DCT-based filter to filter off the recessive features of the test image. As shown in Figure 2, the recessive features are usually reserved for high-frequency areas of the image, while the dominant features are reserved for low-frequency areas. Through DCT transform-domain method, we transform spatial-domain image pixels into frequency-domain coefficients and separate the dominant features from the recessive features. By discarding coefficients of high-frequency areas, the filter could filter off most of recessive features. A DCT-based filter is illustrated in Figure 3. The details of the filter are listed below. The implementation of the filter is presented in Algorithm 2.

(1) Executing two-dimensional DCT, the  $M \times N$  image  $x$  is transformed into an  $M \times N$  matrix  $xf$  of frequency-domain coefficients;

(2) Setting feature reservation ratio  $\alpha$ , and generating a dominant feature matrix  $lf$  by reserving low-frequency coefficients and setting all of high-frequency coefficients to 0 in matrix  $xf$ ;

(3) Executing the inverse of two-dimensional DCT, the matrix  $lf$  is transformed into a mutant image  $xm$ , which reserves most of the dominant features and removes a great number of the recessive features.

---

**Algorithm 2: The Implementation of the Filter**

---

**Input:** Test image  $x$ , feature reservation ratio  $\alpha$   
**Output:** Mutant image  $xm$

1	$xf = \text{DCT}(x)$	← Transform a test image into a frequency-domain matrix by 2-D DCT
2	$lf = \text{zeros\_like}(xf)$	← Initialize an array of zeros with the same shape as a given matrix $xf$
3	<b>for</b> $i = 0$ <b>to</b> $\text{int}(M \cdot \alpha)$ <b>do:</b>	← Reserve the low-frequency coefficients of the array $xf$
4	<b>for</b> $j = 0$ <b>to</b> $\text{int}(N \cdot \alpha)$ <b>do:</b>	
5	$lf[i,j] = xf[i,j]$	
6	<b>end for</b>	
7	<b>end for</b>	
8	$xm = \text{IDCT}(lf)$	← Transform $lf$ into a mutant image by inverse 2-D DCT

---

## V. EXPERIMENTAL EVALUATION

### A. Performance of DCT-based Filter

The design of the feature-filter roots from an explanation for the existence of adversarial examples, that is, recessive features are involved in neural network decisions. It is critical for the feature-filter to filter off recessive features of the test image. In our work, the dominant features and the recessive features are defined from a human-centric perspective. Therefore, the feature-filter should generate mutant images which are still clearly recognizable to humans.

To test the DCT-based filter, we set feature reservation ratio  $\alpha = 0.5$ , which means 3/4 of the frequency features are filtered off by the DCT-based filter. As shown in Figure 4, five random test images are entered into the DCT-based filter and we obtain their mutant images. Even if most of the high-frequency features are moved by the DCT-based filter, human eyes still clearly identify test images and mutant images as the same category. It indicates that the moved features are not perceived by the human eyes.

Whether the DCT-based filter can reliably filter off recessive features from the test image? To verify the performance of the DCT-based filter, we conducted an extensive user study based on human eye evaluation. In the test, the DCT-based filter generates 300 mutant images at multiple feature reservation ratios, which are from 30 benign images in 10 categories in ILSVRC2012 ImageNet dataset [45]. We recruit a total of 50 participants to label these mutant images. For each trail, mutant images are shown on the screen at a fixed size and the order of images is random. In ILSVRC2012 ImageNet dataset, each image contains more than one object, and only one object category is labeled in each image. In order to clarify ambiguity in evaluation, we design the following test.

**Test:** Each participant is required to label 300 mutant images generated by the DCT-based filter. The participants are allowed to identify multiple (up to 5) objects in an image. As long as one of the objects indeed corresponded to the ground-truth label, this mutant image would be judged to reserve the enough dominant features. We calculate the proportion of trails where mutant images are labeled as a ground-truth label. Higher proportion denotes better performance of the DCT-based filter.

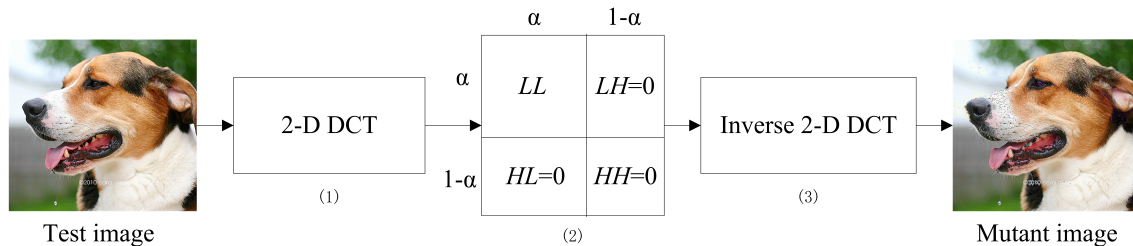


Fig. 3: Overview of the DCT-based Filter.

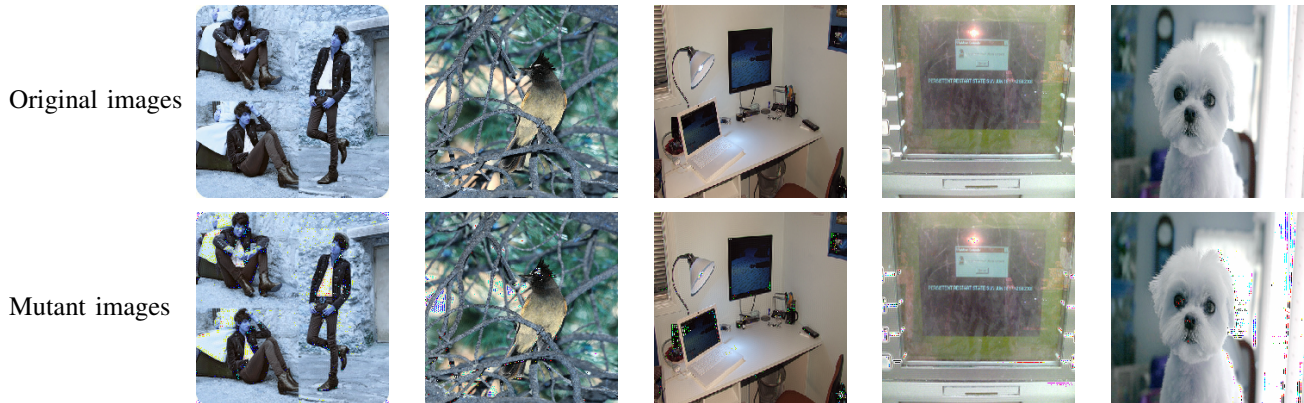


Fig. 4: Performance of the DCT-based Filter.

**Results:** Table I lists the proportion of mutant images being labeled correctly at 5 feature reservation ratios  $\alpha$ . Most of the mutant images are still recognizable to human eyes, which indicates human eyes are not sensitive to the high-frequency features of images. In particular, when  $\alpha = 0.5$ , i.e. 3/4 of the high-frequency features are removed, the proportion of the mutant images correctly recognized is as high as 95.13%. That is to say, human eyes rarely use high-frequency features to understand images. We also observe that the proportion slowly increases as  $\alpha$  increases, which denotes the high-frequency features only contain a small number of comprehensible features to humans (dominant features). The results show that the DCT-based filter can reliably filter off recessive features from the test image.

TABLE I: Proportion of Mutant Images That Are Correctly Labeled by Human Eyes.

$\alpha$	Proportion
0.9	<b>98.73%</b>
0.8	98.33%
0.7	97.67%
0.6	96.53%
0.5	95.13%

### B. Detection against C&W Attack

The premise of the feature-filter design is that the attacker’s perturbations enrich recessive features, yet hardly affect dominant features. In order to test its detection performance, we need to generate a set of very imperceptible adversarial examples. Among state-of-the-art adversarial attacks, C&W

attack is proven to be a more powerful attack, in which  $L_2$  attack can generate higher quality adversarial examples. C&W attack can bypass multiple types of detectors. Similar results are reported in the literature [47] where C&W attack bypassed all of the ten detection methods. Therefore, we focus on our experiments with the challenging C&W attack ( $L_2$  norm) on the CIFAR-10 over Carlini network [25] and ImageNet over Inception V3.

We evaluate the feature-filter from true-positive rate (TPR) and true-negative rate (TNR). TPR measures the proportion of adversarial examples that are correctly identified by the detector while TNR measures the proportion of benign examples that are correctly identified by the detector. The experiment randomly select 500 CIFAR-10 adversarial examples and 50 ImageNet adversarial examples generated by C&W attack to compute TPR and TNR. Notes that the results exclude the failed adversarial examples and over-fitting examples from consideration.

Table II lists the results of TPR and TNR at multiple feature reservation ratios  $\alpha$ . In the best case, the detection rate of adversarial examples is as high as 98.20% for CIFAR-10 when  $\alpha = 0.8$  and 100.00% for ImageNet when  $\alpha = 0.7$ . In addition, we also observe that TNR decreases as  $\alpha$  decreases, which is consistent with the facts that more feature loss reduces the accuracy of neural networks.

We compare the feature-filter with previous adversarial detection approaches based on image transformation, e.g., bit depth reduction [41], spatial smoothing (local smoothing and non-local smoothing) [41], and rotation [42]. Table III lists the results of TPR and TNR for several detectors built upon single transformation on the CIFAR-10 dataset. The results

TABLE II: TPR and TNR at Multiple Feature Reservation Ratios  $\alpha$ .

$\alpha$	CIFAR-10		ImageNet	
	TPR	TNR	TPR	TNR
0.95	97.00%	<b>98.80%</b>	72.00%	<b>100.00%</b>
0.90	<b>98.20%</b>	97.00%	84.00%	100.00%
0.85	97.80%	96.80%	96.00%	100.00%
0.80	98.20%	94.20%	98.00%	100.00%
0.75	98.00%	92.60%	98.00%	100.00%
0.70	98.20%	89.20%	<b>100.00%</b>	98.00%
0.65	97.00%	83.00%	100.00%	98.00%
0.60	95.60%	79.20%	100.00%	90.00%
0.55	96.60%	69.60%	100.00%	92.00%
0.50	96.20%	66.00%	100.00%	90.00%

show that DCT transform is a more effective approach than other image transformation to distinguish adversarial examples from benign examples.

TABLE III: Comparison of TPR and TNR Based on Several Image Transformation on CIFAR-10.

Approaches	Parameters	TPR	TNR
Feature-Filter	0.90	<b>98.20%</b>	<b>97.00%</b>
	0.80	98.20%	94.20%
	0.70	98.20%	89.20%
	0.60	95.60%	79.20%
	0.50	96.20%	66.00%
Bit Depth Reduction	1-bit	89.15%	45.11%
	2-bit	92.22%	78.31%
	3-bit	<b>93.88%</b>	92.69%
	4-bit	89.00%	97.52%
	5-bit	85.75%	<b>98.76%</b>
Median Smoothing	2×2	<b>95.09%</b>	<b>82.03%</b>
	3×3	94.07%	66.17%
	4×4	89.80%	43.87%
Non-local Mean	11-3-2	86.30%	99.25%
	11-3-4	<b>92.73%</b>	96.41%
	13-3-2	89.72%	<b>99.26%</b>
	13-3-4	90.63%	97.03%
Rotation	-20	88.48%	60.22%
	-10	91.60%	84.01%
	10	<b>93.33%</b>	<b>85.50%</b>
	20	91.17%	65.30%

We employ the Receiver Operating Characteristic (ROC) curve and the corresponding Area Under Curve (AUC) to evaluate the detection performance of the feature-filter on the CIFAR-10 dataset. Figure 5 plots the ROC curves for several detectors on the task of detecting adversarial images. Table IV lists the AUC values for several detectors based on image transformation.

The high detection rate shows that filtering off recessive features could significantly change DNN's prediction labels of imperceptible adversarial examples. The results suggest that recessive features of misleading DNNs result in imperceptible adversarial examples, and adversarial attack is essentially a

kind of method to enrich these recessive features in the image.

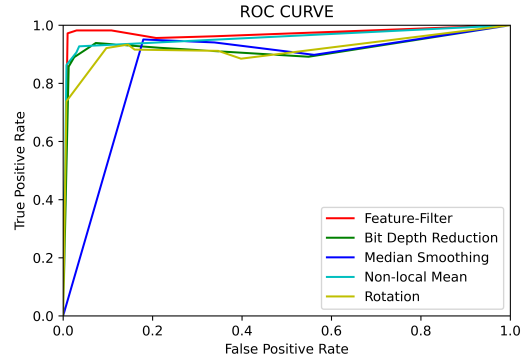


Fig. 5: Comparison of ROC Curves.

TABLE IV: Comparison of AUC Values.

Approaches	AUC
Feature-Filter	<b>96.23%</b>
Bit Depth Reduction	92.18%
Median Smoothing	85.70%
Non-local Mean	95.76%
Rotation	91.95%

### C. Natural Noise Detection

Adversarial examples are a kind of images with special noises, while there are a large number of images with natural noise in reality. A good adversarial examples detector should be able to tolerate natural noises, which would identify natural noise examples to be benign rather than adversarial.

The section focus on verifying whether our detector can correctly identify natural noise images as benign ones. We add 3 types of noises, e.g., Gaussian, Poisson, and salt&pepper to generate natural noise images. The natural noise detection performance is evaluated on a pre-trained Inception V3 [7] model in the ILSVRC2012 ImageNet classification task. Notes that the natural noises here refer to the perturbations which do not change the prediction of the neural network, so that distinguishing it from the adversarial perturbations.

Table V lists the accuracy of the feature-filter in detecting 3 types of natural noise images. Due to existing of multiple objects in an image of the ImageNet dataset, We test top-1 and top-5 to evaluate our detector performance on natural noise images. Higher accuracy denotes better tolerance of the detector to the natural noise. As shown in Table V, the top-5 accuracy is significantly higher than that of the top-1. Particularly, the top-5 accuracy of the feature-filter is close to 95% for Poisson noise. And our detector shows an approximate performance for 3 types of natural noises, which can stably avoid the interference of natural noise. We also see that the accuracy of the feature-filter slowly decreases as  $\alpha$  decreases. The phenomenon reveals that high-frequency features only contain a small amount of dominant features. Therefore, the DCT-based filter could be regarded as a reliable tool to filter off the recessive features from the test image.

TABLE V: Natural Noise Detection on ILSVRC2012 ImageNet.

$\alpha$	Gaussian		Poisson		Salt&Pepper	
	Top-1	Top-5	Top-1	Top-5	Top-1	Top-5
0.95	<b>79.42%</b>	<b>93.31%</b>	<b>80.87%</b>	<b>94.68%</b>	<b>79.29%</b>	<b>93.62%</b>
0.90	79.19%	93.20%	79.76%	94.59%	75.61%	93.01%
0.85	78.08%	92.93%	79.50%	94.18%	73.98%	90.94%
0.80	79.38%	92.20%	79.42%	93.37%	74.64%	89.77%
0.75	79.13%	92.47%	79.29%	94.05%	72.32%	88.67%
0.70	77.72%	91.53%	78.38%	93.21%	71.78%	87.92%
0.65	77.51%	91.39%	77.52%	92.45%	71.29%	88.24%
0.60	74.60%	91.23%	75.90%	91.05%	71.33%	88.79%
0.55	73.08%	89.76%	75.67%	90.85%	70.05%	88.28%
0.50	70.79%	88.62%	72.53%	89.66%	67.62%	86.19%

#### D. Case Study

Why does the feature-filter based on two-dimensional DCT more advantageous? To answer this question, we conduct the case study for two adversarial images in Figure 6 that can be successfully detected by our detector but cannot be detected by other methods (bit depth reduction and median smoothing).

As we explained above in Section I, the imperceptibility of the adversarial example is due to the inconsistency between the features utilized by the human eye and neural networks in image classification. Adversarial attacks would try to enrich recessive features to trick the DNN-based classifier without changing dominant features. Therefore, adversarial detections based on image transformation should compress the space of recessive features as much as possible without the loss of dominant features. A subjective way to evaluate the performance of such detectors is to compress more image features without perceptual loss. In order to display clear perceptual loss, we detect adversarial examples generated by the C&W attack on the  $299 \times 299$  ImageNet.

For DCT-based filter, we set the feature reservation ratios  $\alpha = 0.7$ , which means that only 49% features are retained and 51% features are filtered off. For bit depth reduction, the bit depth is set to 4, which means that 50% features are filtered off. Median smoothing is a method of modifying image features, not filtering off them. Among the three methods, DCT-based filter removes more image features.

Figure 6 shows that the human eye can hardly perceive the difference between benign images and adversarial images, which indicates C&W only enrich recessive features of two case images. We separately perform image transformations on case adversarial samples and get their mutant images (sub-figure (c, d, g, and h)). As shown in Figure 6, even if more features are filtered off, the mutant images based on the feature-filter have less visible artifacts than other approaches. The results indicates that the removed features are almost recessive. Feature-filter can compress the space of recessive features with less perceptual loss.

#### E. Computation Cost

Apart from detection rate, efficiency is also an important parameter for a good adversarial detector. The feature-filter consists of a filter, a predictor and a discriminator. The filter is

based on two-dimensional DCT to generate the mutant image of the test image. As defined in Equations 5 and 6, the time complexity of DCT and its inverse transform is  $O(M \times N)$  for an  $M \times N$  image. The predictor is made up of the target DNN, which performs two predictions on the test image and its mutant image. Thus, computation cost of the predictor depends on the efficiency of the neural network. The discriminator only gives the decision according to two predicted labels by the predictor, thus its time complexity is  $O(1)$ .

The actual running time depends on many factors including experimental setup, programming skill, etc. Our test is implemented on an Intel Core I5 CPU 2.30 GHz, NVIDIA GeForce GTX 1060 and 8.0 GB of RAM computer that run on Windows 10 and Spyder (Python 3.6). We choose 1,000 random images to test the running time of the feature-separator. The average running time is 0.0351 second for a  $224 \times 224 \times 3$  ImageNet image and 0.0028 second for a  $32 \times 32 \times 3$  CIFAR-10 image. Due to the low computation cost, the feature-separator could be a real-time adversarial detector.

#### CONCLUSION

The explanation of adversarial example phenomenon remains an open issue. As a human-centric phenomenon, we divide the image feature into dominant features and recessive features. We reveal that the existence of imperceptible adversarial examples is due to the DNN’s use of the recessive features. Adversarial attacks attempt to enrich the recessive features of the input so that the perturbed example can “fool” the DNN and hardly result in noticeable artifacts.

According to above explanation, adversarial examples should be more sensitive to the operation of filtering off recessive features than benign/noisy examples. Inspired by this idea, we propose an adversarial detection approach named feature-filter. The feature-filter determines whether the test image is adversarial by comparing the DNNs prediction labels on the test input and its mutant that is filtered off recessive features. To filtering out recessive features, we introduce two-dimensional DCT to separate the dominant features and the recessive features. The experimental results show that the DCT-based filter can reliably filter off the recessive features from the image, and the feature-filter is a label-only tool to detect adversarial examples.

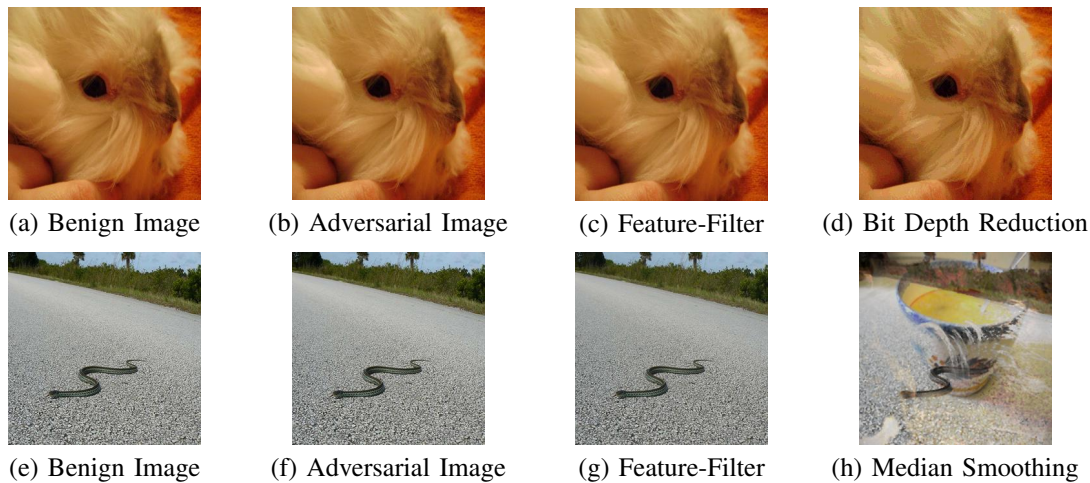


Fig. 6: Loss of Dominant Features.

The effectiveness of the feature-filter stems from a reliable filtering of recessive features. As discussed in Section V, two-dimensional DCT is an approximate method to separate the recessive features from the dominant features. Future works are to discover more reliable feature filtering methods or combine the feature-filter with other methods, so that the adversarial detector is more accurate and robust.

#### ACKNOWLEDGMENT

This work was supported by National Natural Science Foundation of China (Grants No. U1936122).

#### REFERENCES

- [1] K. He, X. Zhang, S. Ren, and J. Sun, Deep residual learning for image recognition, *IEEE Conference on Computer Vision and Pattern Recognition (CVPR)*, pp. 770-778, 2016.
- [2] G. Huang, Z. Liu, L. Maaten, and K. Weinberger, Densely connected convolutional networks, *IEEE Conference on Computer Vision and Pattern Recognition (CVPR)*, pp. 4700-4708, 2017.
- [3] S. Karen, Z. Andrew. Very deep convolutional networks for large-Scale image recognition, *International Conference on Learning Representations (ICLR)*, pp. 1-14, 2015.
- [4] J. Hu, L. Shen, S. Albanie, G. Sun, and E. Wu, Squeeze-and-Excitation networks, *IEEE Conference on Computer Vision and Pattern Recognition (CVPR)*, pp. 7132-7141, 2018.
- [5] R. Blanco-Gonzalo, O. Miguel-Hurtado, C. Lunerti, R. Guest, B. Corsetti, E. Ellavarason, and R. Sanchez-Reillo, Biometric systems interaction assessment: The state of the art, *IEEE Transactions on Human-Machine Systems*, vol. 49, no. 5, pp. 397-410, 2019.
- [6] Y. Mirsky, T. Doitshman, Y. Elovici, and A. Shabtai, Kitsune: An ensemble of autoencoders for online network intrusion detection, *arXiv preprint arXiv:1802.09089*, 2018.
- [7] C. Szegedy, V. Vanhoucke, S. Ioffe, J. Shlens, and Z. Wojna, Rethinking the inception architecture for computer vision, *IEEE Conference on Computer Vision and Pattern Recognition (CVPR)*, pp. 2818-2826, 2016.
- [8] C. Szegedy, W. Zaremba, I. Sutskever, J. Bruna, D. Erhan, I. Goodfellow and R. Fergus, Intriguing properties of neural networks, *arXiv preprint arXiv:1312.6199*, 2013.
- [9] I. Goodfellow, J. Shlens, and C. Szegedy, Explaining and harnessing adversarial examples, *arXiv preprint arXiv:1412.6572*, 2014.
- [10] A. Rozsa, E. M. Rudd, T. Boult, et al, Adversarial diversity and hard positive generation, *IEEE Conference on Computer Vision and Pattern Recognition (CVPR)*, pp. 410-417, 2016.
- [11] X. Yuan, P. He, Q. Zhu, and X. Li, Adversarial examples: Attacks and defenses for deep learning, *IEEE Transactions on Neural Networks and Learning Systems*, vol. 30, no. 9, pp. 2805-2824, 2019.
- [12] S-M. Moosavi-Dezfooli, A. Fawzi, and P. Frossard, Deepfool: A simple and accurate method to fool deep neural networks, *IEEE Conference on Computer Vision and Pattern Recognition (CVPR)*, pp. 2574-2582, 2016.
- [13] S-M. Moosavi-Dezfooli, A. Fawzi, O. FAWZI O, and P. Frossard, Universal adversarial perturbations, *IEEE Conference on Computer Vision and Pattern Recognition (CVPR)*, pp. 86C94, 2017.
- [14] J. Dong, S. Ji, T. Du, B. Li and T. Wang, Textbugger: Generating adversarial text against real-world applications, *Network and Distributed System Security Symposium (NDSS)*, pp. 1-15, 2019.
- [15] A. Bhattad, M. Chong, K. Liang, B. Li and D. A. Forsyth, Unrestricted adversarial examples via semantic manipulation, *International Conference on Learning Representations (ICLR)*, pp. 1-20, 2020.
- [16] J. Su, D-V. Vargas and K. Sakurai, One-pixel attack for fooling deep neural networks, *IEEE Transactions on Evolutionary Computation*, vol. 23, no. 5, pp. 828-841, 2019.
- [17] C. Laidlaw, S. Singla and S. Feizi, Perceptual adversarial robustness: Defense against unseen threat models, *arXiv preprint arXiv:2006.12655*, 2020.
- [18] F. Chiaroni, M.C. Rahal, N. Hueber and F. Dufaux, Self-supervised learning for autonomous vehicles perception: A conciliation between analytical and learning methods, *IEEE Signal Processing Magazine*, vol. 38, no. 1, pp. 31-41, 2021.
- [19] X. Xu, J. Zhang, Y. Li, Y. Wang, Y. Yang and H. T. Shen, Adversarial attack against urban scene segmentation for autonomous vehicles, *IEEE Transactions on Industrial Informatics*, vol. 17, no. 6, pp. 4117-4126, 2021.
- [20] K. Pei, Y. Cao, J. Yang, and S. Jana, Deepxplore: Automated whitebox testing of deep learning systems, *ACM Symposium on Operating Systems Principles*, pp. 1-18, 2017.
- [21] Uri Shaham, Yutaro Yamada, and Sahand Negahban, Understanding adversarial training: Increasing local stability of supervised models through robust optimization, *Neurocomputing*, vol. 307, pp. 195C204, 2018.
- [22] A. Kurakin, I. Goodfellow, and S. Bengio, Adversarial machine learning at scale, *arXiv preprint arXiv:1611.01236*, 2017.
- [23] F. Tram, A. Kurakin, N. Papernot, I. Goodfellow, D. Boneh, and P. McDaniel, Ensemble adversarial training: Attacks and defenses, *International Conference on Learning Representations (ICLR)*, 2018.
- [24] N. Papernot, P. McDaniel, X. Wu, S. Jha, and A. Swami, Distillation as a defense to adversarial perturbations against deep neural networks, In *IEEE Symposium on Security and Privacy (SP)*, 2016.
- [25] N. Carlini, and D. Wagner, Towards evaluating the robustness of neural networks, In *IEEE Symposium on Security and Privacy (SP)*, 2017.
- [26] G. Cohen, G. Sapiro, and R. Giryes, Detecting adversarial samples using influence functions and nearest neighbors, *IEEE Conference on Computer Vision and Pattern Recognition (CVPR)*, pp. 14453-14462, 2020.
- [27] S. Bubeck, E. Price, and I. Razenshteyn. Adversarial examples from computational constraints. *arXiv preprint arXiv:1805.10204*, 2018.
- [28] A. Shafahi et al. Are adversarial examples inevitable? *International Conference on Learning Representations (ICLR)*, pp. 1-17, 2019.
- [29] S. Mahloujifar, D. I. Diochnos, and M. Mahmoody. The curse of concentration in robust learning: Evasion and poisoning attacks from

- concentration of measure, AAAI Conference on Artificial Intelligence (AAAI), pp. 1-24, 2018.
- [30] A. Ilyas, S. Santurkar, D. Tsipras, L. Engstrom, B. Tran, and A. Madry, Adversarial examples are not bugs, they are features, arXiv preprint arXiv: 1905.02175, 2019.
- [31] Z. Yahya, M. Hassan, S. Younis, and M. Shafique, Probabilistic analysis of targeted attacks using transform-domain adversarial examples, IEEE ACCESS, vol. 8, pp. 33855-33869, 2020.
- [32] G. K. Dziugaite, Z. Ghahramani, and D. M. Roy, A study of the effect of JPG compression on adversarial images, arXiv preprint arXiv: 1805.10204, 2018.
- [33] N. Das, M. Shanbhogue, S. Chen, F. Hohman, L. Chen, M. E. Kounavis, and D. H. Chau. Keeping the bad guys out: Protecting and vaccinating deep learning with jpeg compression. arXiv preprint arXiv:1705.02900, 2017.
- [34] N. Papernot, P. McDaniel, A. Sinha, and M. Wellman, SoK: towards the science of security and privacy in machine learning, IEEE European Symposium on Security and Privacy (EuroS&P), pp. 399-414, 2018.
- [35] N. Papernot, P. McDaniel, X. Wu, S. Jha, and A. Swami, Distillation as a defense to adversarial perturbations against deep neural networks, IEEE Symposium on Security and Privacy (S&P), pp. 582-597, 2016.
- [36] G. Cohen, G. Sapiro, and R. Giryes, Detecting adversarial samples using influence functions and nearest neighbors, IEEE Conference on Computer Vision and Pattern Recognition (CVPR), pp. 14453-14462, 2020.
- [37] R. Feinman, R. R. Curtin, S. Shintre, and A. B. Gardner, Detecting adversarial samples from artifacts, arXiv preprint arXiv: 1703.00410, 2017.
- [38] P. Yang, J. Chen, C. Hsieh, J. Wang, and M. I. Jordan, ML-LOO: detecting adversarial examples with feature attribution, AAAI Conference on Artificial Intelligence (AAAI), PP. 6639-6647, 2020.
- [39] S. Ma, Y. Liu, G. Tao, W. Lee, and X. Zhang, NIC: detecting adversarial samples with neural network invariant checking, Network and Distributed Systems Security Symposium (NDSS), pp. 1-15, 2019.
- [40] P. Sperl, C. Kao, P. Chen, and K. Bottinger, DLA: dense-layer-analysis for adversarial example detection, IEEE Symposium on Security and Privacy (EuroS&P), pp. 1-21, 2020.
- [41] W. Xu, D. Evans, and Y. Qi, Feature squeezing: detecting adversarial examples in deep neural networks, Network and Distributed Systems Security Symposium (NDSS), pp. 1-15, 2018.
- [42] S. Tian, G. Yang, and Y. Cai, Detecting adversarial examples through image transformation, AAAI Conference on Artificial Intelligence (AAAI), pp. 4139-4146, 2018.
- [43] Y. Kantaros, T. Carpenter, S. Park, R. Ivanov, S. Jang, I. Lee, and J. Weimer, VisionGuard: Runtime detection of adversarial inputs to perception systems, arXiv preprint arXiv: 2002.09792, 2020.
- [44] Y. Bahat, M. Irani, and G. Shakhnarovich, Natural and adversarial error detection using invariance to image transformations, arXiv preprint arXiv: 1902.00236, 2019.
- [45] O. Russakovsky, J. Deng, H. Su, J. Krause, S. Satheesh, S. Ma, Z. Huang, A. Karpathy, A. Khosla, M. Bernstein, A. C. Berg and L. Fei-Fei, ImageNet large scale visual recognition challenge, International Journal of Computer Vision, col. 115, no. 3, pp. 211C252, 2015.
- [46] H. Dai, J. Cheng, and Y. Li, A novel steganography algorithm based on quantization table modification and image scrambling in DCT domain, International Journal of Pattern Recognition and Artificial Intelligence, vol. 35, no. 1, pp. 1-18, 2021.
- [47] N. Carlini, and D. Wagner, Adversarial examples are not easily detected: bypassing ten detection methods, arXiv preprint arXiv: 1705.07263, 2017.